Mechatronics and Automation Technology
J. Xu (Ed.)
© 2022 The authors and IOS Press.
This article is published online with Open Access by IOS Press and distributed under the terms of the Creative Commons Attribution Non-Commercial License 4.0 (CC BY-NC 4.0).
doi:10.3233/ATDE221160

Multi-Exposures with Dose Modulation of SU-8 Based on DMD Maskless Lithography for PDMS (Dimethylsiloxane) Microchannels

Qiming CHEN[a,1], Xianwen SONG[a], Renxuan FU[a], Junqi GAN[b], Jinyun ZHOU[c], Yibiao LIU[a] and Yongjun XU[a]
[a] *School of Mechanical and Electrical Engineering, Guangdong Polytechnic of Industry and Commerce, Guangzhou, 510510, China*
[b] *School of Automotive Engineering, Guangdong Polytechnic of Industry and Commerce, Guangzhou, 510510, China*
[c] *School of Physics and Optoelectronic Engineering, Guangdong University of Technology, Guangzhou,510006, China*

Abstract. A multi-exposures with dose modulation method is presented to fabricate SU-8 mold which is used for microfluidic channels. The method used a maskless digital lithography device with a 405 nm LED source. Digital micromirror device (DMD) maskless lithograph can reach higher precision to meet the requirements of microfluidic chips. For a thick SU-8 layer, multi-exposures with low dose method can effectively suppress the T-shaped structure formed due to top overexposed and bottom underexposed. Two SU-8 molds were fabricated with 55 μm and 25 μm in height in this work. The number of exposures is 62 and 55, respectively. The actual contour of SU-8 structures closely matches the design contour. The PDMS microchannel structure was fabricated using the SU-8 mold. The minimum width of a single microchannel achieved 10 μm. This method provides a more flexible method for fabricating SU-8 molds with higher precision and is well suited for on-chip cell isolation.

Keywords. Multi-exposures, Dose modulation, DMD, SU-8, PDMS microchannel.

1. Introduction

Microchannels have been widely used in microfluidics. Microfluidics offers the possibility of system miniaturization and integration for the rapidly expanding field of biomedical diagnostics, biological assays, and drug discovery[1-3]. A microfluidic chip is a miniaturized system with microchannels that can transport trace reagents for separation, treatment, and detection[4-6]. Microchannels are traditionally fabricated by 3D printing technology, which involves layer-by-layer stacking technology, for

[1] Corresponding Author, Qiming CHEN, School of Mechanical and Electrical Engineering, Guangdong Polytechnic of Industry and Commerce, Guangzhou, 510510, China; Email: chqmpku@gdgm.edu.cn.

example, stereo lithography apparatus (SLA). The SLA performs layer-by-layer with a certain thickness exposure curing of the photosensitive resin by the electromechanically controlled, and layers are stacked to form a three-dimensional structure. The structure exists problems such as edge discontinuities and overall structural deformation because of the non-uniform release of intermolecular stress between layers. The precision of traditional stereolithography is limited to 50 μm[7] The size of common animal and human cells is between 10-40 μm. For example, human mesenchymal cells have dimensions of around 20 μm[8]，while human cervical carcinoma cells (HeLa cells) are about 10 μm in size[9]. Microchannels fabricated by traditional lithography cannot achieve such precision. Digital micromirror device (DMD) maskless lithography techniques[10-12] have the advantages of greater precision and lithographic flexibility in fabricating microchannels, which can meet the requirement. In recent years, soft polymers have become the most popular materials for microchannel fabrication due to their excellent chemical and physical properties as well as their biocompatibility[13]. PDMS is one such polymer that has become a common material for microchannel fabrication. This material has several distinct advantages, including electrical insulation, nontoxicity, optical transparency and chemical inertness[14]. During the fabrication process, a master mold fabricated from SU-8[15] photoresist is usually prepared. The SU-8 exposure light source is usually the high-power mercury lamp I-line (365 nm)[16-19] which has the disadvantages of high power consumption, short life, large spectral range, pollution, etc. According to the Beer-Lambert's law[20], For a thick photoresist layer, when the high power UV light illuminated from top to bottom, the intensity is weakened, therefore the top is easily over-exposed and the bottom is underexposed. This situation leads to form a T-shaped structure which reduced lithography quality[21-22]. LED light source is widely used in maskless lithography system due to its advantages of single spectrum, long life, no pollution, low power, and energy saving. Since DMD havs the best light transmission efficiency for 400-420 nm wavelengths light [23], the generic light source of DMD maskless lithography is a center wavelength of 405 nm LED light source.

In this article, we propose a method to fabricate the SU-8 mold by using the multiple exposure with dose modulation method on one-time spin-coated photoresist. This method effectively avoids the formation of T-shaped structures while improving the precision of the microfluidic single channel. The actual contour of the manufactured SU-8 structure closely matches the design contour, and the smallest width of single PDMS microchannel fabricated by using this SU-8 structure reach 10 μm, which is a breakthrough.

2. Experimental Section

2.1. Graphic Design

Figure 1 shows a diagram of the DMD digital lithography device. The main components are the DMD chip, the light source and the reflection device. The light source is a 405 nm LED. This light source is converted into the exposure light with high collimation and uniform illumination by a series of condenser lens. Then the exposure light is projected onto a DMD microchip through a reflecting mirror. The chip is made by Texas Instruments. DMD chip has a full-field resolution of 2048×1024 pixels. The size of the single micromirror is 10.8×10.8 μm². The rotation angle of the DMD is 7.125°. After the DMD chip and a microlens array (MLA) deflection, the exposure light is focused by the objective lens and projected onto the substrate.

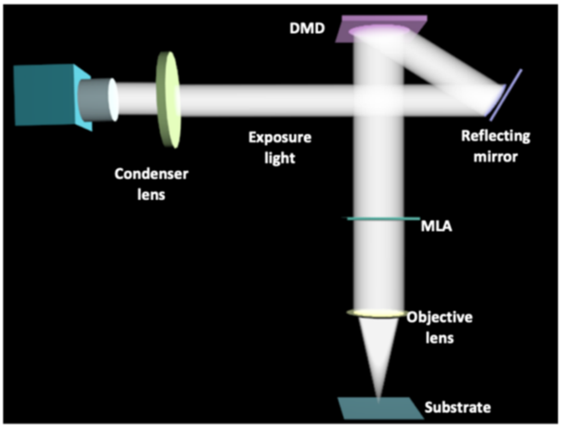

Figure 1. Diagram of DMD maskless lithography device.

Considering cell isolation applications, two types of splitter microfluidic channels were designed as shown in figure 2 using a software called L-Edit. Figure 2(a) is a splitter named pattern A with four branch channels. The linewidths of the four channels are 10, 20, 30, and 40 μm; The diameters of the corresponding four reservoirs are 20, 30, 40, and 50 μm respectively. Figure 2(b) is a splitter named pattern B with a main channel that narrows from 40 μm to 10 μm. The size of the four reservoirs is the same with pattern A.

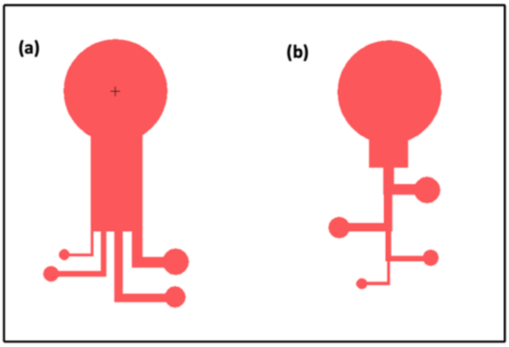

(a) 4 branches splitter. (b) Main channel narrowing splitter

Figure 2. The schematic of the digital mask patterns

2.2. Exposure Principle and Process

As shown in figure 3, the fabrication process of three-dimensional PDMS microfluidic channels involves spin coating, soft bake, optical exposure, baking, development, molding and thermal crosslinking. EPON Resin SU-8 series photoresists are spin-coated in thicknesses ranging from 25 μm to 225 μm. The photoresist is EPON resin by the type SU-8 2050. The thickness of the spin coating corresponds to the depth of the micro channel. The channel 55 μm in deep is close to the size of the cell, which is a suitable depth. The photoresist we used is SU-8 which is a kind of negative photoresist. The spin coated thickness ranges from 25 μm to 150 μm. The substrate we used is a Cr plate (2 inch×2 inch, 1 inch=2.54 cm). To allow more uniform coating of the SU-8 photoresist on the substrates, both substrates were pretreated by baking at 120°C for 10 minutes, followed by cooling for 5 minutes. After that, one sample was first spin-coated with the photoresist at 600 rpm for 10 s, then spin-coated at 2600 rpm for 40 s. Next, the sample was soft baked as shown in figure 3(a) in order to improve the adhesion. Finally, the substrate was cool for 30 minutes. A layer of approximately 55 μm in thickness SU-8 was obtained. As a comparison, another sample was spin-coated 40 s at 4000 rpm, the rest of the process was the same as above. We obtain a SU-8 layer 25 μm in thickness.

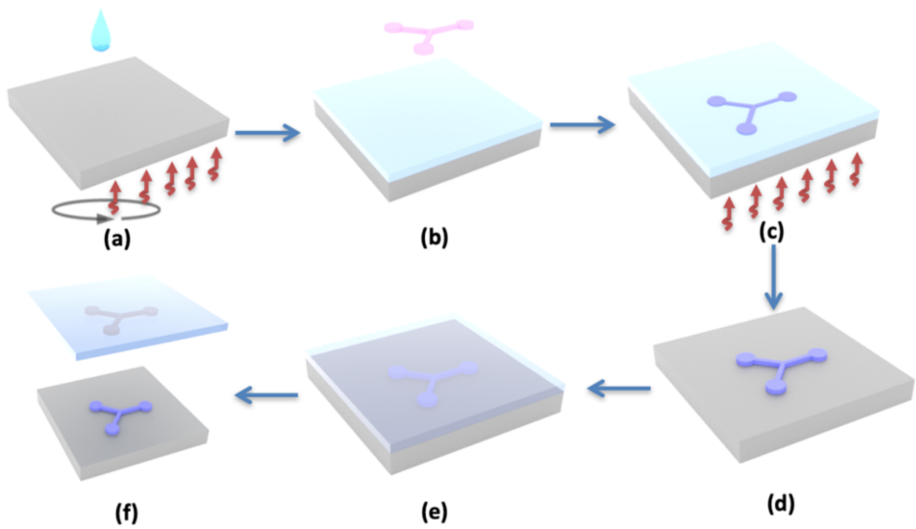

(a) spin-coating, (b) exposure, (c) bake, (d) development, (e) molding, (f) thermally crosslinking

Figure 3. Schematic diagrams of processing flows of three-dimensional PDMS microfluidic channel

For a negative photocurable resin, it has exposure thresholds E_{th} and E_c. E_{th} is defined as the minimum exposure dose required for the initial reaction of the resin. E_c is the exposure dose required for maximum curing height. There is a contrast γ value, which is related to the exposure dose and the thickness of the photoresist, as shown in Eq (1) [24].

$$\gamma = \frac{1}{\ln E_c - \ln E_{th}} = \frac{h}{H[\ln E - \ln E_{th}]} \tag{1}$$

where $0 \le h \le H$, $E_{th} \le E \le E_c$. h and H represent the exposure height and theoretical the maximum height, respectively. From Eq. (1), we derive he following equation:

$$E = \exp\left(\frac{h}{H\gamma} + \ln E_{th}\right) \tag{2}$$

E_{th} and E_c of the SU-8 series photoresist are 150 mJ/cm^2 and 350 mJ/cm^2, respectively. The contrast γ is equal to 1.18. The maximum theoretical spin coated height H is 225 μm. The relationship between h and the required exposure dose E can be calculated according to Eq. (2). The result is shown in figure 4. When h=55 μm, the theoretical calculated exposure dose is 184.4 mJ/cm^2. When h=25 μm, the calculated exposure dose is 164.7 mJ/cm^2.

The exposure dose J is defined as:

$$J=I\bullet T \tag{3}$$

In the formula, I represents the light intensity, T represents the exposure time. We create a multi-exposure with dose modulation method which is equivalent to using low light intensity and increasing the exposure time to let the exposure dose reach the value.

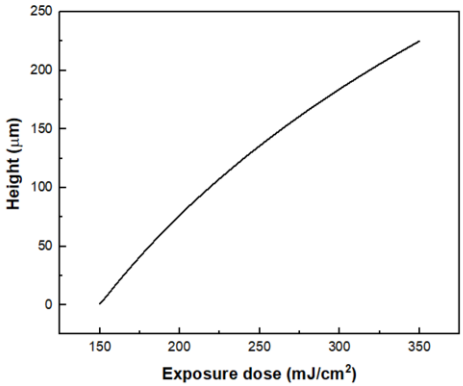

Figure 4. The relationship between exposure dose and height of SU-8 series photoresist.

The maximum exposure dose is 3 mJ/cm^2 at once time in our device. In order to verify the calculation results, 55 μm thick sample was repeat-exposed 62 times and 25 μm thick sample was repeat-exposed 55 times, as shown in figure 3(b). during the repeat-exposed process, Each SU-8 sample remains in the same position. The sample does not need to be taken out and the position offset is negligible.

After exposure, the substrates were post-baked 1min at 65°C ,then heated to 95°C for 15 min as shown in figure 3(c), and then soaked in the developer solution for 6 min. Finally, the samples were hard baked 30 min at 150°C and nitrogen dried for increasing stiffness. The designed graphics are saved as shown in figure 3(d).

2.3. Microchannel Fabrication

After that, the PDMS microfluidic channels were made using molding and thermal cross-linking technology. First, curing agent and PDMS were mixed in a 1:10 ratio. In order to mix well, the mixture was left for 5 min. And then degassed in a vacuum chamber for 30 min. After that it was poured onto two SU-8 molds and solidified in an oven at 70°C for 24 h, as shown in figure 3(e). Both PDMS membranes with micro channels were gently peeled from the molds as shown in figure 3(f). Both PDMS membranes were ultrasonically cleaned using N, N-dimethylformamide for 5 minutes. Finally, both membranes were glued to two slides.

3. Results and Discussions

To evaluate the morphologies and heights of the molds, both SU-8 molds were investigated using 3D laser-scanning confocal microscopy (LSCM). A set of LSCM results of SU-8 mold fabricated by repeat-exposed 62 times are presented in figure 5. The laser image of pattern A is presented in figure 5(a). One can see that the pattern is convex and intact. Figure 5(b) showed a 2D optical image of the full pattern A. The mold is nearly 1 mm in length and 500 microns in width. The edge of the silhouette is also very sharp. This SU-8 mold is ideal for fabricating PDMS microfluidic chips. the height of SU-8 corresponds to the depth of the microchannel. Therefore, the height was measured. The result is presented in figure 5(c). In figure 5(c), one can see that the mold is 55 µm in height which is consistent with the calculated result as presented in figure 4. Additionally, each channel's height is nearly the same, which demonstrates that the multi-exposure process was successful. The widths of the channels are 10, 20, 30, and 40 µm, and the interval between each channel is 30 µm which is the same as the virtual mask. Figure 5 (d) is the laser image of the 3D structure of the SU-8 mold fabricated with pattern B. The mold is convex, and the edge of the profile is smooth. Height measurement results are shown in figure 5(e) and 5(f) The same colors in 5(e) represent the same heights. The green line indicates the measuring line. The height is 55 µm as required. From the results above, it is clear that the sidewalls are almost vertical and no "T" shape. The profile is clearly outlined at the convex and concave corners. This indicates that the multi-exposure method effectively prevents the formation of the T-shaped structures.

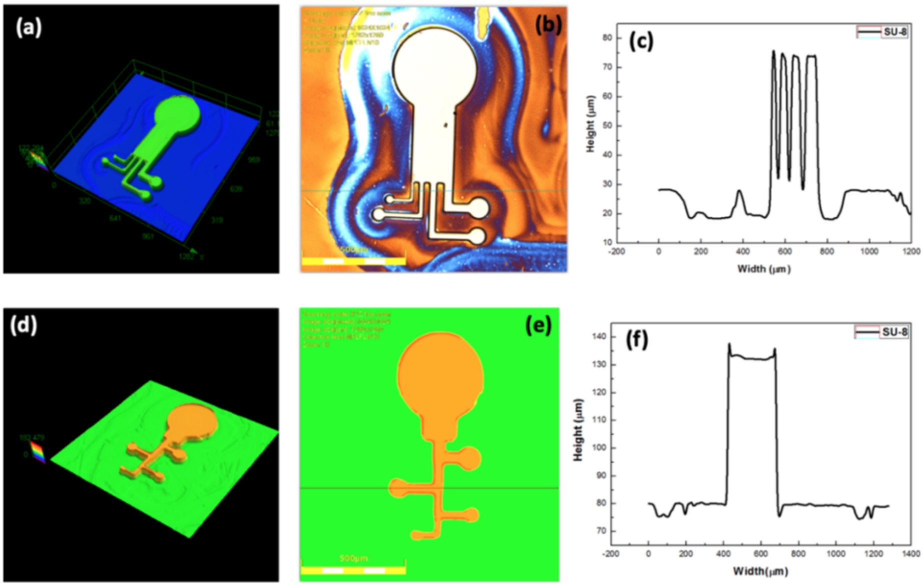

Figure 5. LSCM images of the repeat-exposed 62 times SU-8 mold, for pattern A: (a) 3D image, (b) 2D image, (c) height measurement for pattern B: (d) 3D image, (e) 2D image, (f) height measurement

The morphological characteristics of the PDMS microchannels fabricated by the SU-8 mold above were also investigated by using LSCM, as demonstrated in figure 6. The laser image of the 3D structure of the PDMS microfluidic channel is presented in figure 6(a). It can been seen that the channels are concave and clear. The PDMS microfluidic chip is an inverse pattern. Figure 6(b) displayed a PDMS microfluidic channels 2D image. One can see that the pattern has been copied perfectly. Every microchannel is clear and no impurities. The depths of the channels were measured using LSCM, as shown in figure 6(b) and 6(c). The result in figure 6(c) told that the depths of the four channels are found to be exactly at 55 μm except for the narrowest channel in which some impurities remain. Figure 6(d) is the laser image of the 3D structure of the pattern B microchannel. The pattern is convex, the edge of the profile is smooth. Figure 6(e) and 6(f) show the depth measurement of the mold. From figure 6(f), one can see that the main channel narrows and has a depth of 55 μm. The results showed that we successfully fabricated PDMS microchannels.

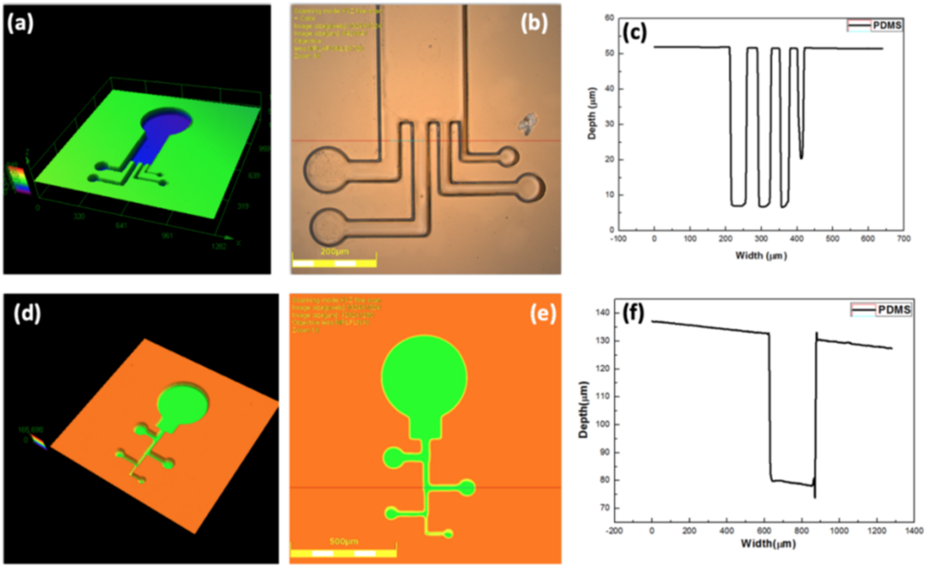

Figure 6. LSCM image of two kinds of 55 μm deep PDMS microchannel, for pattern A: (a) 3D image, (b) 2D image, (c) depth measurement, for pattern B: (d) 3D image, (e) 2D image, (f) depth measurement

Figure 7 is a set of LSCM graphs of 55 repeat-exposures. The laser image of the 3D structure of type A is presented in figure 7(a). One can see that the pattern is convex. Figure 7(b) displayed the full 2D optical image of type A. Every microchannel is clear. The result of the height measurement is presented in figure 7(c). In figure 7(c), one can see that the SU-8 mold is 25 μm in height which is consistent with the calculated result as represented in figure 4.The result demonstrates that the repeat exposure process was successful. The widths of the channels are 10, 20, 30, and 40 μm, and the interval between each channel is 30 μm which is the same as the virtual pattern. Figure 7(d) is the laser image of the 3D structure of pattern B mold. The height of the entire mold is uniform as indicated by the color. Figure 7(e) and 7(f) show the height measurements of the mold. The sidewalls are also vertical and no “T” shape.

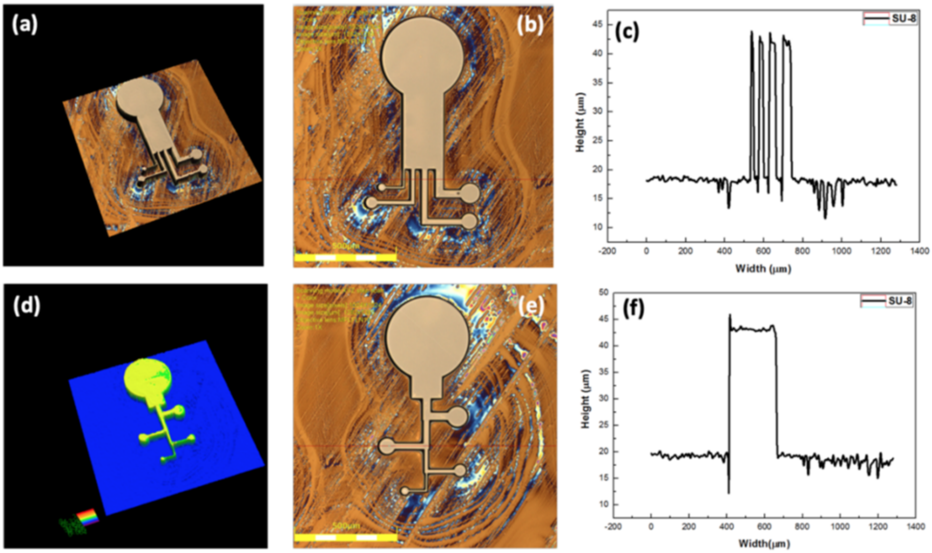

Figure 7. LSCM images of the repeat-exposed 55 times SU-8 mold, for pattern A: (a) 3D image, (b) 2D image, (c) height measurement for pattern B: (d) 3D image, (e) 2D image, (f) height measurement

Figure 8(a) is a laser image of the PDMS microchannels fabricated by the SU-8 mold with 25 μm in height. It can been seen that t the channels are clear. Figure 8(b) is a 2D graph of the microchannels. Every channel is clear and no impurities. The depths of the channels were measured using LSCM, as shown in figure 8(b) and 8(c). The result in figure 8(c) told that the depths of the four channels are found to be exactly the same at 25 μm. Figure 8(d) is the laser image of the 3D structure of pattern B microchannel. The pattern is convex, and the edge of the profile is smooth. Figure 8(e) and 8(f) display the depth measurement of the microchannel. From figure 8(f), one can see that the main channel has a depth of 25 μm.

We also did a comparative experiment. For a SU-8 layer with 25 μm in thickness, when exposures number is less than 55, the bottom of SU-8 is underexposed, resulting in the pattern detachment during development. When the number of exposures is more than 55, the top of SU-8 is overexposed and a T-shaped structure appears. These results demonstrate that the minimum number of exposures is the same as we calculated. Therefore, we summarize the relationship between the number of exposures and the desired SU-8 thickness, as shown in figure 9. When the thickness of SU-8 increases, we can find the corresponding exposure times to fabricate high-quality SU-8 molds.

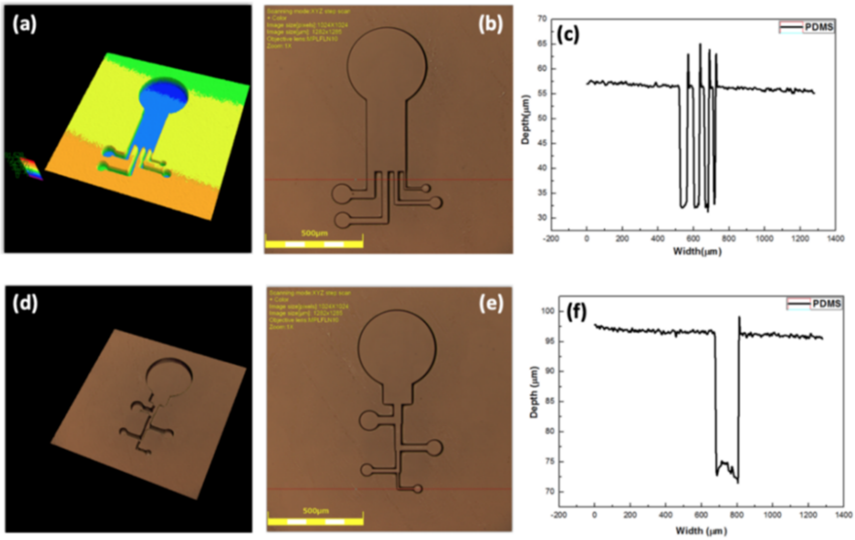

Figure 8. LSCM image of two kinds of 25 μm deep PDMS microchannels, for pattern A: (a) 3D image, (b) 2D image, (c) depth measurement, for pattern B: (d) 3D image, (e) 2D image, (f) depth measurement

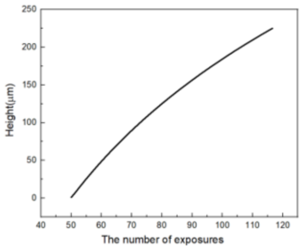

Figure 9. The relationship between number of exposures and height of SU-8 series photoresist.

4. Conclusions

A dose-modulated multi-exposures method on one-shot spin-on photoresist was developed to fabricate SU-8 molds by DMD maskless lithography with the light source 405 nm in wavelength. PDMS microchannels were then fabricated using SU-8 molds. We reach the following conclusion: the generation of T-shaped structures is effectively avoided by the method of multi-exposures; the width of a single channel reaches 10 μm through DMD maskless lithography and we find the relationship between the number of exposures and the thickness of SU-8. This method provides a more flexible method for fabricating the SU-8 mold with higher precision and will have a wide range of applications in the field of microfluidics.

Acknowledgements

This study was supported by Guangzhou Science and Technology Planning Project (grant no. 202102021302) and Foundation for High-Level Talents in Higher Education of GDPIC (No. 2021-gc-03,2021-gc-04).

References

[1] Dittrich, P.S. & Manz, A. Lab-on-a-chip: microfluidics in drug discovery, Nat. Rev. Drug Discov. 2006, 5:210–218.

[2] Fang, X., Chen, H., Xu, L., Jiang, X., Wu, W. & Kong, J. A portable and integrated nucleic acid amplification microfluidic chip for identifying bacteria. Lab Chip, 2012, 12: 1495–1499.

[3] Guo, M.T., Rotem, A., Heyman, J.A. & Weitz, D.A. Droplet microfluidics for high-throughput biological assays. Lab Chip, 2012, 12: 2146–2155.

[4] Nagrath, S., Sequist, L.V., Maheswaran, S., Bell, D.W., Irimia, D., Ulkus, L., Smith, M.R., Kwak, E. L., Digumarthy, S., Muzikansky, A. & Ryan, P. Isolation of rare circulating tumor cells in cancer patients by microchip technology. Nature, 2007, 450: 1235–1239.

[5] Tung, Y.C., Huang, N.T., Oh, B.R., Patra, B., Pan, C.C., Qiu, T., Chu, P.K., Zhang, W.& Kurabayashi, K. Optofluidic detection for cellular phenotyping. Lab Chip, 2012, 12: 3552–3565.

[6] Huang, N.T., Zhang, H. L., Chung, M.T., Seo J. H.& Kurabayashi, K. Recent advancements in optofluidics-based single-cell analysis: optical on-chip cellular manipulation, treatment, and property detection. Lab Chip, 2014, 14: 1230–1245.

[7] Shallan, A. I., Smejkal, P., Corban, M., Guijt, R.M. & Breadmore, M.C. Cost-effective three-dimensional printing of visibly transparent microchips within minutes Anal. Chem, 2014, 86: 3124.

[8] Gao, S., Tung, W.T., Wong, D. S. H., Bian L. & Zhang, A. P. Direct optical micropatterning of poly(dimethylsiloxane) for microfluidic devices[J]. Micromech. Microeng, 2018, 28: 095011.

[9] Zhai, Z. M., Zhang, F. Q., Chen, X.Y., Zhong, J., Liu, G., Tian Y.C. & Huang, Q. Uptake of silver nanoparticles by DHA-treated cancer cells examined by surface-enhanced Raman spectroscopy in a microfluidic chip. Lab Chip, 2017, 17: 1306.

[10] Totsu, K., Fujishiro, K., Tanaka, S. & Esashi, M. Fabrication of three-dimensional microstructure using maskless grayscale lithography. Sensors Actuators A, 2006, 130–1, 387–92.

[11] Xiang, N., Yi, H., Chen, K., Wang, S. & Ni Z. Investigation of the maskless lithography technique for the rapid and cost-effective prototyping of microfluidic devices in laboratories [J]. Micromech. Microeng. 2013, 23: 025016.

[12] Luo, N. & Zhang, Z. Fabrication of a curved microlens array using double gray-scale digital maskless lithography[J]. Micromech. Microeng. 2017, 27: 035015.

[13] Waldbaur, A., Rapp, H., Länge, K.& Rapp, B. E. Let there be chip—towards rapid prototyping of microfluidic devices: one-step manufacturing processes. Anal. Methods, 2011, 3: 2681–716.

[14] McDonald, J. C. & Whitesides, G.M. Poly(dimethylsiloxane) as a material for fabricating devices Acc. Chem. Res, 2002, 35: 491–9.

[15] Huang, B.B., Yin, M.J., Zhang A.P. & Ye, X.S. On-chip microfabrication of thermally controllable PNIPAAm microvalves by using optical maskless stereolithography Sens. Actuators A: Physical, 2016, 247: 397–402.

[16] Wu, J., Guo, X., Zhang, A. P. & Tam, H.Y. Rapid 3D μ-printing of polymer optical whispering-gallery mode resonators. Optics Express, 2015, 23: 29708-29714.

[17] Yin, M. J., Yao, M., Gao, S., Zhang, A.P., Tam, H.Y.& Wai, P. K. A. Rapid 3D Patterning of Poly (acrylic acid) Ionic Hydrogel for Miniature pH Sensors. Advanced Materials, 2016, 28: 1394-1399.

[18] Yin, M. J., Huang, B.B., Gao, S.R., Zhang, A.P. & Ye, X. S. Optical fiber LPG biosensor integrated microfluidic chip for ultrasensive glucose detection Biomedical Optics Express **7**, 2067, (2016).

[19] Wang, J., Yao, M., Hu, C. Z., Zhang, A. P., Shen, Y. H., Tam, H.Y.& A. Wai, P. K. Optofluidic tunable mode-locked fiber laser using a long-period grating integrated microfluidic chip. Optics Letters, 2017, 42: 1117.

[20] Mack, C.A., Matsuzawa, T., Sekiguchi, A. &Minami, Y. Resist metrology for lithography simulation, part I: exposure parameter measurements. Proc. SPIE Metrology, Inspection, and Process Control for Microlithography X , 1996, 2725, 34-48.

[21] Xu, B.J., Jin, Q.H. & Zhao, J.L. Fabrication and application of multilayer SU-8 based micro dispensing array chip, Journal of Functional Materials and Devices, 2006, 12: 377-382.

[22] Zhao, L., Zhang, B.Z., Duan, J.P. & Cui, J.L. The design and manufacture of micro cantilever based on thick photoresist, Science Technology and Engineering, 2015, 15, 128-131.

[23] www. ti.com

[24] Kemhadjian, H. Microlithography: Science and Technology, Int. J. Electr. Eng. Educ. 2007, 36:275-276.